

Phenomenology of Non-Custodial Warped Models

Adrián Carmona,¹ Eduardo Pontón,² and José Santiago¹

¹ *CAFPE and Departamento de Física Teórica y del Cosmos,
Universidad de Granada, E-18071 Granada, Spain*

² *Department of Physics, Columbia University,
538 W. 120th St, New York, NY 10027, USA*

(Dated: August 17, 2011)

Abstract

We study the effect of bulk fermions on electroweak precision observables in a recently proposed model with warped extra dimensions and no custodial symmetry. We find that the top-quark mass, together with the corrections to the $Zb_L\bar{b}_L$ vertex and the one-loop contribution to the T parameter, which is finite, impose important constraints that single out a well defined region of parameter space. New massive vector bosons can be as light as ~ 1.5 TeV and have large couplings to the t_R quark, and suppressed couplings to the t_L , b_L and lighter quarks. We discuss the implications for searches of models with warped extra dimensions at the LHC.

I. INTRODUCTION

Models with warped extra dimensions [1] are excellent candidates for physics beyond the Standard Model. They solve the hierarchy problem, provide a rationale for the observed flavor structure, and can potentially give striking signatures at the LHC. Besides, they are weakly coupled duals of strongly coupled four-dimensional (conformal) theories and can therefore provide an intuition and quantitative predictions for models of strong electroweak symmetry breaking (EWSB).

Models based on a purely AdS_5 background and a minimal field content are strongly constrained by electroweak precision tests (EWPT). In particular, large contributions to the Peskin-Takeuchi T parameter [2] can easily push the scale of new physics beyond the reach of the LHC [3]. The large top mass requires the third generation $SU(2)_L$ quark doublet (as well as the top singlet) to be relatively close to the infrared (IR) brane. When the light generations are localized near the ultraviolet (UV) brane, this can lead to large corrections to the $Zb_L\bar{b}_L$ coupling, which also impose important restrictions. A common solution invokes a custodial symmetry [4], and a benchmark model of anarchic warped extra dimensions was proposed in Ref. [5] (see [6] for alternatives). In that model, the S parameter –together with the one-loop fermion contributions to T and the $Zb_L\bar{b}_L$ coupling [7], which are calculable in such models–imposes the strongest constraint: the new vector bosons should be heavier than 3–4 TeV.¹ The couplings of the quarks to these Kaluza-Klein (KK) vector bosons in the previous benchmark model were taken to be

$$g_{t_R} \sim 5g_{SM} , \quad g_{t_L}, g_{b_L} \sim g_{SM} , \quad g_q \sim -g_{SM}/5 , \quad (1)$$

where q represents any of the light Standard Model (SM) fermions and g_{SM} represents a typical SM couplings. The conclusion of LHC reach studies is that the gauge KK resonances are difficult to see at the LHC, mainly due to their large width and reduced production cross section, the latter resulting from the small coupling to valence quarks [5, 9]. Luckily, this benchmark model comes with another characteristic signature: light vector-like fermions (fermion custodians) [10], that are much easier to see at the LHC [11] (see [12] for an overview).

It has been recently suggested [13] that a departure from pure AdS_5 near the infrared brane

¹ If one gives up on the anarchy assumption, the constraints can be significantly relaxed [8].

can substantially decrease the T parameter (and, although by a smaller amount, also the S parameter, as was previously observed in [14, 15]). The authors of [13] proposed a model in which the reduction of the T and S parameters is so effective that new vector bosons with masses below 1 TeV are compatible with the EWPT *without the custodial symmetry*. The analysis in [13] assumes, however, that all fermions are localized on the UV brane. This is an excellent approximation for the light generations but not for the third one.

We extend the previous study by incorporating bulk fermions and describing their effects on EWPT once the top and bottom masses are reproduced. This is important for a number of reasons: first, without the custodial symmetry the $Zb_L\bar{b}_L$ coupling is not protected [4] and can impose significant constraints on the model; second, the loop-level contributions to the EW observables are expected to be strongly dependent on the localization of the third family of quarks, and can also impose significant constraints; finally, the collider implications of the model depend crucially on the localization of the third generation quarks. Nevertheless, we find that the signatures associated with the region of parameter space favored by the EW precision constraints are still characterized by Eq. (1), although lighter resonances than in the AdS_5 background may be allowed.

The outline of the paper is as follows. We introduce the model in Section II and discuss bulk fermions in Section III. The EW constraints of the model are investigated in Section IV and its collider implications in Section V. We conclude in Section VI.

II. A WARPED MODEL WITHOUT CUSTODIAL SYMMETRY

The model under consideration represents a departure from AdS_5 in the infrared. We simply summarize in this section the main results for the gravitational background and the bosonic field content, while referring the reader to [13] for full details. We will then introduce bulk fermions in the model and discuss their effects on the EWPT. The gravitational background is given by the metric

$$ds^2 = e^{-2A(y)}\eta_{\mu\nu}dx^\mu dx^\nu - dy^2, \quad (2)$$

with warp factor

$$A(y) = ky - \frac{1}{\nu^2} \log\left(1 - \frac{y}{y_s}\right). \quad (3)$$

The extra dimension is bounded by two branes: the UV brane, localized at $y = 0$, and the IR brane, localized at $y = y_1$. The warp factor would vanish at y_s but we will always consider parameters such that this metric singularity remains hidden behind the IR brane ($y_s > y_1$).

The gravitational parameters are therefore ν , y_1 , y_s and k (the curvature scale at the UV brane, of the order of the Planck mass) which is assumed to set the scale of all dimensionful 5D quantities. We will trade y_s for the value of the curvature radius at the IR brane, given in units of k by

$$kL_1 = \frac{\nu^2 k (y_s - y_1)}{\sqrt{1 - 2\nu^2/5 + 2\nu^2 k (y_s - y_1) + \nu^4 k^2 (y_s - y_1)^2}} . \quad (4)$$

Requiring perturbativity of the gravitational expansion bounds its value by $kL_1 \gtrsim 0.2$ [13]. The position of the IR brane, y_1 , can be fixed by requiring the gravitational background to generate the M_P/TeV hierarchy. We will simply set $A(y_1) = 35$, which determines y_1 .

The bosonic content of the model consists of the SM gauge fields, with Neumann boundary conditions (BC) on both branes, and an electroweak scalar doublet, the Higgs. Other scalars involved in the gravitational background and the stabilization of the interbrane distance [13] are irrelevant for this discussion, although their phenomenology, in particular that of the radion, can be interesting. The bulk gauge bosons can be expanded in KK modes (we focus on the μ component here, which is the relevant one for EWPT and collider implications):

$$A_\mu(x, y) = \frac{1}{\sqrt{y_1}} \sum_n f_n^A(y) A_\mu^{(n)}(x) , \quad (5)$$

where the profiles satisfy

$$[\partial_y e^{-2A} \partial_y + m_n^2] f_n^A = 0 , \quad \partial_y f_n^A|_{y=0, y_1} = 0 , \quad (6)$$

(we treat EWSB perturbatively), and are normalized according to

$$\frac{1}{y_1} \int_0^{y_1} dy f_n^A f_m^A = \delta_{nm} . \quad (7)$$

The boundary conditions fix the value of the KK masses. They are of the order of the effective IR scale

$$\tilde{k}_{\text{eff}} \equiv A'(y_1) e^{-A(y_1)} , \quad (8)$$

i.e. of order the warped down curvature at the IR brane. We show in Fig. 1 the mass of the first gauge KK mode, in units of \tilde{k}_{eff} , for different values of ν and kL_1 .

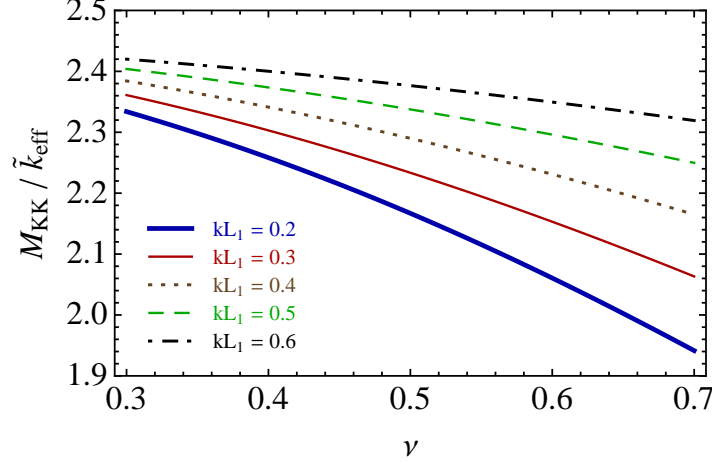


FIG. 1: Mass of the first gauge KK mode in units of the effective IR scale \tilde{k}_{eff} , defined in Eq. (8), as a function of ν and for different values of kL_1 .

For the Higgs field we can write

$$H(x, y) = \frac{1}{\sqrt{2}} e^{i\chi(x, y)} \begin{pmatrix} 0 \\ h(y) + \xi(x, y) \end{pmatrix}, \quad (9)$$

where the Higgs KK expansion reads

$$\xi(x, y) = \frac{1}{\sqrt{y_1}} \sum_n f_n^\xi(y) \xi^{(n)}(x), \quad (10)$$

and the wavefunctions are normalized to

$$\frac{1}{y_1} \int_0^{y_1} dy e^{-2A} f_n^\xi f_m^\xi = \delta_{nm}. \quad (11)$$

For a light Higgs we can assume that the Higgs vacuum expectation value (vev) is carried by the zero-mode, which has a profile

$$f_0^\xi(y) \approx N_h e^{aky}, \quad (12)$$

with N_h fixed by the normalization condition (11). Following [13] we trade a for

$$\delta \equiv \left| e^{-2(a-2)ky_s} ky_s [-2(a-2)ky_s]^{-1+\frac{4}{\nu^2}} \Gamma\left(1 - \frac{4}{\nu^2}, -2(a-2)k(y_s - y_1)\right) \right|, \quad (13)$$

which is a measure of how much fine-tuning in the 5D parameters we need to impose in order to preserve the Randall-Sundrum solution to the hierarchy problem [1].

In summary, we have two free parameters for the gravitational background, ν and kL_1 ; and one for the Higgs background, δ . However the EWPT are quite insensitive to the latter so we will simply fix $\delta = 0.1$ in the following.

III. BULK FERMIONS

We introduce now bulk fermions in the model. The quadratic part of the action for bulk fermions reads

$$S = \int d^4x dy e^{-4A} \bar{\Psi} \left[e^A i \not{\partial} + (\partial_5 - 2A') \gamma^5 - M \right] \Psi , \quad (14)$$

where M is a 5D Dirac mass allowed by the symmetries. Following the standard procedure we expand the bulk fermions in KK modes

$$\Psi_{L,R}(x, y) = \frac{1}{\sqrt{y_1}} \sum_n f_n^{L,R}(y) \psi_{L,R}^{(n)}(x) , \quad (15)$$

where we have defined the 4D chiralities $\Psi_{L,R} = \frac{1}{2}(1 \mp \gamma^5)\Psi$, and the KK profiles satisfy the following system of equations:

$$\begin{aligned} [\partial_y - (2A' + M)] f_n^R &= -e^A m_n f_n^L , \\ [\partial_y - (2A' - M)] f_n^L &= e^A m_n f_n^R , \end{aligned} \quad (16)$$

with the ortho-normality conditions given by

$$\frac{1}{y_1} \int_0^{y_1} dy e^{-3A} f_n^L f_m^L = \frac{1}{y_1} \int_0^{y_1} dy e^{-3A} f_n^R f_m^R = \delta_{nm} . \quad (17)$$

Bulk fermions with a left-handed (LH) zero-mode are obtained by imposing Dirichlet boundary conditions for their right-handed (RH) chirality on both branes. Such bulk fermions will be denoted as “[++] fermions”. The boundary conditions for the opposite, LH, chirality are fixed by the equations of motion. Similarly, bulk fermions with a RH zero-mode are obtained by imposing Dirichlet boundary conditions on their LH chirality, and will be denoted as “[−−] fermions”. The LH (RH) massless profile of a [++] ([−−]) bulk fermion is given by

$$f_0^{L,R}(y) = N_0^{L,R} e^{2A \mp \int_0^y dy' M(y')} , \quad (18)$$

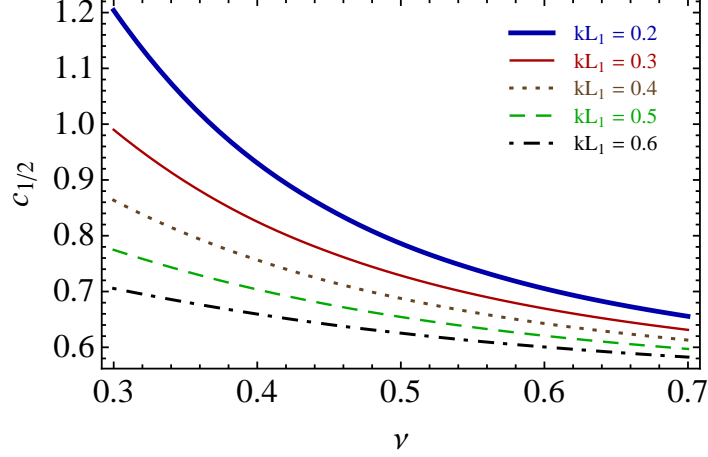


FIG. 2: Value of the localization parameter, $c_{1/2}$, that makes a LH fermion zero-mode mostly delocalized, as a function of ν and for different values of kL_1 .

where $N_0^{L,R}$ is fixed by the normalization condition. In the following we will consider a constant bulk mass $M_i = c_i k$, where i denotes the fermion type.²

In the present metric background there are no exactly flat fermion solutions, unlike for a pure AdS_5 background, $A_{\text{RS}}(y) = ky$, with a constant 5D Dirac mass defined by $c = 1/2$. However, the c parameter does control the localization of the fermion zero-modes, either towards the IR or UV brane. In particular, there is always a background-dependent value, $c_{1/2}$, such that for $c < c_{1/2}$, the (LH) fermion zero-mode is mostly IR localized, while for $c > c_{1/2}$ it is mostly UV localized. This value plays a role analogous to $c = 1/2$ in the pure AdS_5 background. In Fig. 2 we show the value of $c_{1/2}$, defined such that $e^{-\frac{3}{2}A(0)}f_0^L(0) = e^{-\frac{3}{2}A(y_1)}f_0^L(y_1)$ (see Eq. (24) and footnote 5), as a function of the input parameters ν and kL_1 (see also Fig. 7).

Let us now discuss the couplings of the fermion zero-modes to the Higgs and gauge boson KK modes in this model. The gauge couplings are given by

$$\begin{aligned} \mathcal{L} &\supset g_5 \int dy e^{-3A} \bar{\Psi} \not{A} \Psi = \sum_{mnr} \frac{g_5}{\sqrt{y_1}} \int dy e^{-3A} \frac{f_n^L f_m^L f_r^A}{y_1} \bar{\psi}_L^{(n)} \not{A}^{(r)} \psi_L^{(m)} + (L \rightarrow R) \\ &\equiv \sum_{mnr} g_{nmr}^L \bar{\psi}_L^{(n)} \not{A}^{(r)} \psi_L^{(m)} + (L \rightarrow R), \end{aligned} \quad (19)$$

² In the limit in which $y_s \rightarrow y_1$ there could be problems of strong coupling similar to the ones present in soft-wall models [15], and a y -dependent mass term might be necessary [16] (see [17] for other realizations of flavor in soft-wall models).

whereas the Yukawa couplings can be computed from

$$\begin{aligned} \mathcal{L} &\supset Y_5 \int dy e^{-4A} \bar{Q}_L H U_R + (L \leftrightarrow R) \\ &= \sum_{mn} \frac{Y_5}{\sqrt{y_1}} \int dy e^{-4A} \frac{f_L^{Q(n)} f_\xi^{(0)} f_R^{U(m)}}{y_1} \bar{q}_L^{(n)} h u_R^{(m)} + (L \leftrightarrow R) + \dots \equiv \lambda_{mn}^{LR} \bar{q}_L^{(n)} h u_R^{(m)} + \dots, \end{aligned} \quad (20)$$

where we have defined $h \equiv \xi^{(0)}(x)$. The 5D gauge coupling can be fixed by matching the coupling of the gauge zero-mode to the observed 4D coupling. Assuming a tree-level matching this gives

$$g_5 = \sqrt{y_1} g_4. \quad (21)$$

For the 5D Yukawa coupling, Ref. [18] finds, based on NDA [19], that its maximum value is given by

$$Y_5 \leq Y_5^{\max} \approx \frac{4\pi}{\sqrt{3k}}, \quad (22)$$

which corresponds to strong coupling at a scale of the third KK level. We plot in the left panel of Fig. 3 the Yukawa coupling between the zero-modes of a $[++]$ fermion Q , and a $[--]$ fermion T , assuming $Y_5 = Y_5^{\max}$, as a function of a common localization parameter $c = c_Q = -c_T$. In the right panel we show the coupling of a LH fermion zero-mode to the first two gauge boson KK modes divided by the coupling to the gauge boson zero-mode (assuming tree level matching) as a function of c . We have chosen $\nu = 0.4$, and $kL_1 = 0.2$ in both plots. We see the change of behavior around $c_{1/2} \approx 0.93$, which corresponds to the most delocalized zero-mode fermion profile (see Fig. 2).

For $c \gtrsim c_{1/2}$, we see that the Yukawa coupling becomes exponentially suppressed. Furthermore, in the same region the coupling to the gauge boson KK modes becomes almost universal (i.e. independent of c). Thus, as for the pure AdS_5 case, the assumption that the light fermions are exactly localized on the UV brane is an excellent approximation (as far as EWPT are concerned) in these models.

IV. ELECTROWEAK CONSTRAINTS

If flavor is explained by means of localization in the extra dimension, the effects of new physics in models with warped extra dimensions are almost universal and can therefore be encoded in the oblique parameters of [20], with the most important exception being the couplings

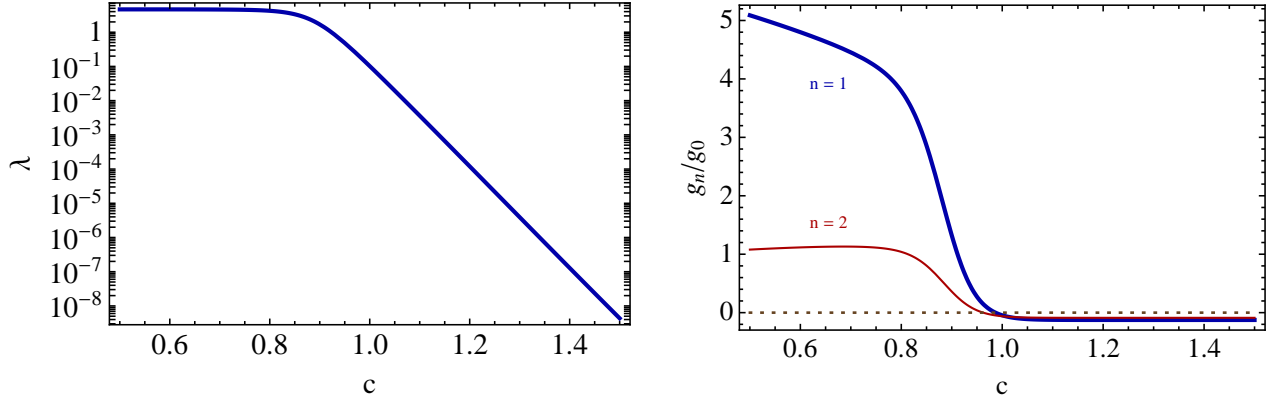


FIG. 3: Left panel: Yukawa coupling, $\lambda \equiv \lambda_{00}^{LR}$, as a function of the bulk mass for $c_L = -c_R = c$ and a 5D Yukawa coupling that saturates the maximum value given in Eq. (22). Right panel: coupling of a LH fermion zero-mode to the first two gauge boson KK modes in units of $g_0 \equiv g_5/\sqrt{y_1}$. In both cases we have taken $\nu = 0.4$ and $kL_1 = 0.2$, which lead to maximally delocalized fermions for $c \approx 0.93$.

of the bottom quark. This can be most easily seen with holographic methods. However, the collider implications of these models are easier to understand if we discuss how the corrections are generated in the physical basis (i.e. the KK-basis). A general discussion of EWPT in models with warped extra dimensions and the equivalence of different methods to compute them is given in [21]. Here we follow the equivalent notation in [13] to make the comparison easier. Before presenting the detailed EW precision analysis, we comment on the calculability of such effects in the present class of models.

A. Calculability

As already emphasized, the present class of models does not have a custodial symmetry to protect the Peskin-Takeuchi T parameter, nor the corrections to certain gauge-fermion couplings. As a result, it is possible to write a term in the bulk that violates the custodial symmetry, $\mathcal{L}_5 \supset (\kappa/\Lambda^3) |H^\dagger D_M H|^2$, where we wrote the coefficient in units of the 5D cutoff, Λ . The dimensionless factor, κ , is UV sensitive. However, when the Higgs propagates in the bulk, the 1-loop contributions are finite by power-counting. To see this, it is simplest to use a normalization where the gauge bosons, W_M , have mass dimension 1 [we write the kinetic term as $(-1/4g_5^2) W_{MN}^a W^{aMN}$]. Then, the contributing diagrams are simply proportional to g_5^4 or

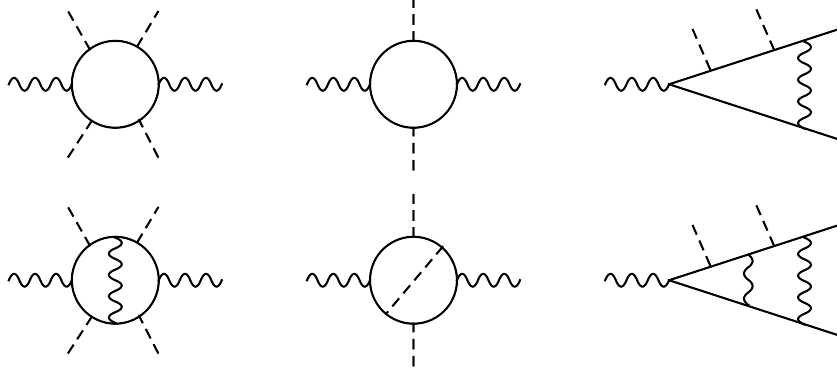


FIG. 4: Examples of radiative corrections to the oblique parameters, as well as to the non-oblique vertex corrections. The most important contributions arise from the top KK-tower in the loop. Upper row, left to right: one-loop contributions to T , S and δg_{b_L} , respectively. Lower row: examples of the corresponding two-loop contributions.

y_5^4 , where both the 5D (top) Yukawa coupling, y_5 , and the 5D gauge coupling have mass dimension $-1/2$. (We show in the upper-left corner of Fig. 4 an example diagram with a fermion loop.) It follows that the piece proportional to $\eta_{\mu\nu}$ in the loop integral has mass dimension -1 , and therefore it is IR dominated. Subtracting the zero-mode contribution, the remainder is controlled by the scale \tilde{k}_{eff} . At two-loop order, an example of which is shown in the lower-left corner of Fig. 4, the diagram is *logarithmically* divergent by power counting.

A similar point has been made in connection to the S -parameter when the Higgs is taken as a bulk field.³ The middle diagram in the upper row of Fig. 4 is finite, while at 2-loop order a *logarithmic* UV sensitivity is encountered (e.g. in the middle diagram of the lower row of Fig. 4), corresponding to the bulk operator $H^\dagger \sigma^a H W_{MN}^a B^{MN}$. Similar remarks apply to “vertex corrections” of the form $(H^\dagger D_M H)(\bar{\Psi} \Gamma^M \Psi)$ or $(H^\dagger \sigma^a D_M H)(\bar{\Psi} \Gamma^M \sigma^a \Psi)$. Examples of 1- and 2-loop contributions to these vertex corrections are shown in the right column of Fig. 4. We also note that operators localized on the branes (corresponding either to T , S or δg_{b_L}) can be induced only at three (and higher-order) loop order.

We conclude that just allowing the Higgs to propagate in the bulk can make the oblique parameters effectively calculable: the incalculable pieces associated with the 5D local operators above are suppressed compared to the finite, one-loop contribution roughly by M_{KK}/Λ . In the

³ K. Agashe, private communication. See also [8].

particular models studied here, the localization properties of the Higgs, to be discussed in the next subsection, imply that the couplings of the Higgs to the KK fermion or gauge states are suppressed compared to the situation in an AdS_5 background. In fact, for the favored region of parameter space such couplings are well in the perturbative regime (thus resembling more closely the case of flat rather than typical warped extra-dimensions). However, although higher-order contributions due to Yukawa or weak gauge couplings can be expected to be further suppressed, there remains some uncertainty associated with higher order QCD contributions. As we will see in detail below, one of the effects of the departure from AdS_5 of the gravitational background is to push the KK modes closer to the IR brane. This effect increases the coupling among KK modes, thus reducing the scale of strong coupling in the QCD sector. This is reminiscent of the position dependent cut-off in soft-wall models [14, 15], and affects the EW observables at two-loop and higher order.⁴ Nevertheless, we find that the finite one-loop contributions to the EW observables –especially to T – can be significant, and therefore one should not neglect such radiative effects. To get a concrete idea about their impact on the EW fit and the resulting bounds on the KK scale, we will assume that the QCD strong coupling scale is high enough to make the 5D description a reasonable approximation. Furthermore we will assume that 2-loop and higher-order QCD effects do not dramatically change the one-loop results. One should, however, keep in mind that QCD effects may not be negligible.

B. The Oblique Corrections at Tree Level

We perform now a detailed analysis of the EW precision constraints in the class of models without custodial symmetries under discussion. In this subsection we focus on the *oblique* analysis at *tree level* (which was already performed in [13]), and in the next one we take the most important non-oblique contribution into account, i.e. the correction to the $Zb_L\bar{b}_L$ coupling, as well as the one-loop contributions. This will allow us to better understand the impact of the various effects. Let us start with the gauge KK-modes. The effects of new physics can be classified in three types: corrections to the gauge boson self-energies, to fermion-gauge

⁴ A smaller hierarchy in the spirit of the Little RS model [22] would reduce the tension with the low QCD cut-off and increase the coupling of the KK-gluon to light quarks, thus having an important impact on collider phenomenology.

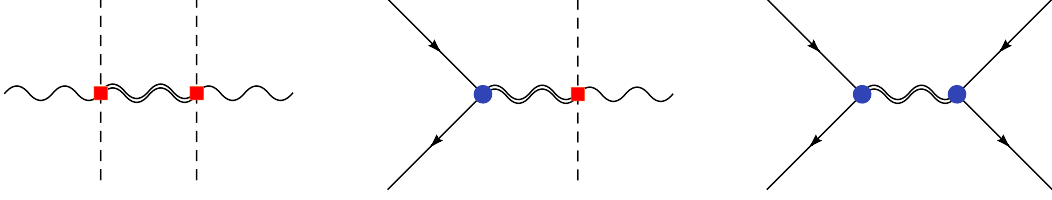


FIG. 5: Contribution to the coefficients $\hat{\alpha}$, $\hat{\beta}$ and $\hat{\gamma}$ of Eq. (24). The double line represents the tower of massive gauge boson KK modes, the red squares the mixing between the gauge KK and zero-modes, and the blue dot the coupling of the light fermions to the gauge KK modes.

couplings and to four-fermion interactions. Each of these effects is characterized by coefficients denoted by $\hat{\alpha}$, $\hat{\beta}$ and $\hat{\gamma}$, respectively. For the present case, only gauge bosons obeying Neumann boundary conditions on both branes are relevant, in which case one has [13]

$$\begin{aligned}\hat{\alpha} &= \int_0^{y_1} dy e^{2A(y)} \left(\Omega_h(y) - \frac{y}{y_1} \right)^2, \\ \hat{\beta} &= \int_0^{y_1} dy e^{2A(y)} \left(\Omega_h(y) - \frac{y}{y_1} \right) \left(\Omega_f(y) - \frac{y}{y_1} \right), \\ \hat{\gamma} &= \int_0^{y_1} dy e^{2A(y)} \left(\Omega_f(y) - \frac{y}{y_1} \right)^2.\end{aligned}\tag{23}$$

The function $\Omega(y)$ is defined by ⁵

$$\Omega_i(y) \equiv \frac{1}{y_1} \int_0^y d\tilde{y} \omega_i(\tilde{y}), \quad \omega_i(y) \equiv \begin{cases} e^{-2A(y)} f_{i,0}^2(y), & \text{scalars} \\ e^{-3A(y)} f_{i,0}^2(y), & \text{fermions} \end{cases},\tag{24}$$

where $f_{i,0}(y)$ is the wave function for the scalar or fermion zero-modes (see previous sections). With our normalization we have $\Omega_i(y_1) = 1$. These coefficients are diagrammatically shown in Fig. 5. The wavy double line represents the tower of *massive* gauge boson KK modes, resummed in Eqs. (24). The blue dot represents the coupling of the SM fermions to the new vector bosons, and the red square the mixing between SM and heavy gauge bosons through Higgs insertions. The oblique parameters due to the KK physics can be written in terms of these coefficients as

$$\hat{T} = \frac{g'^2 v^2}{2} (\hat{\alpha} - 2\hat{\beta} + \hat{\gamma}),\tag{25}$$

$$\hat{S} = g^2 v^2 (-\hat{\beta} + \hat{\gamma}),\tag{26}$$

$$W = Y = \frac{g^2 v^2}{2} \hat{\gamma},\tag{27}$$

⁵ The $\omega_i(y)$ are nothing but the (square of the) “physical wavefunction” profiles, i.e. the profiles with warp factors taken out, as dictated by dimensional analysis (which just redshift all mass scales appropriately).

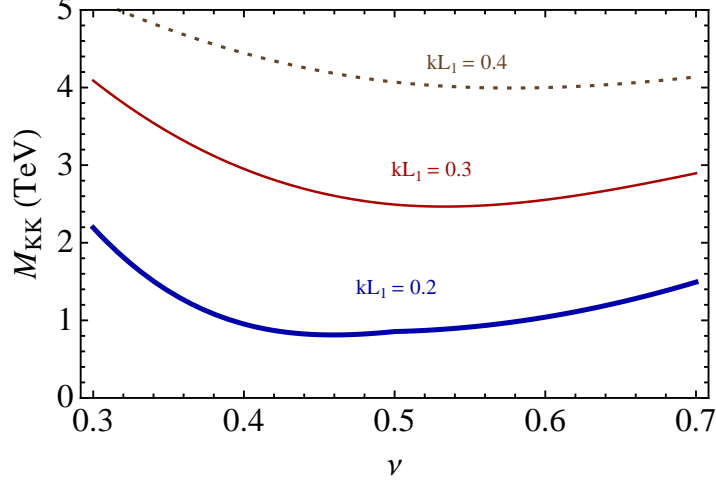


FIG. 6: 95% CL lower bound on the mass of the first KK gauge boson, obtained from a *tree-level oblique* analysis. We assume UV localized fermions and different values of the input parameters ν and kL_1 . See text for details on the fit procedure.

where g and g' are the $SU(2)_L$ and $U(1)_Y$ couplings, respectively, and $v = 174$ GeV is the Higgs vev. These are related to the Peskin-Takeuchi S and T parameters [2] by $\alpha S = 4s_W^2 \hat{S}$ and $\alpha T = \hat{T}$. We also include a Higgs contribution to S and T , given by [23]

$$\Delta S = \frac{1}{2\pi} [g(m_h^2/m_Z^2) - g(m_{\text{ref}}^2/m_Z^2)] , \quad (28)$$

$$\Delta T = -\frac{3}{16\pi c_W^2} [f(m_h^2/m_Z^2) - f(m_{\text{ref}}^2/m_Z^2)] , \quad (29)$$

where

$$g(y) = \int_0^1 dx x(5x-3) \ln(1-x+yx) , \quad (30)$$

$$f(y) = y \frac{\ln c_W^2 - \ln y}{c_W^2 - y} + \frac{\ln y}{c_W^2(1-y)} , \quad (31)$$

and we take $m_{\text{ref}} = 115$ GeV in the fit.

We show in Fig. 6 the result of a fit to the oblique parameters when all fermions are assumed to live on the UV brane for different values of the input parameters ν and kL_1 . We have used an updated version of the code in [24], obtaining the bounds as follows. For fixed values of ν and kL_1 (i.e. for a fixed metric background), we compute the minimum of the χ^2 , including only the Z -pole observables,⁶ as a function of the Higgs mass (imposing the direct LEP bound

⁶ These are the 26 observables associated with the W mass (two measurements), the Z-line shape and lep-

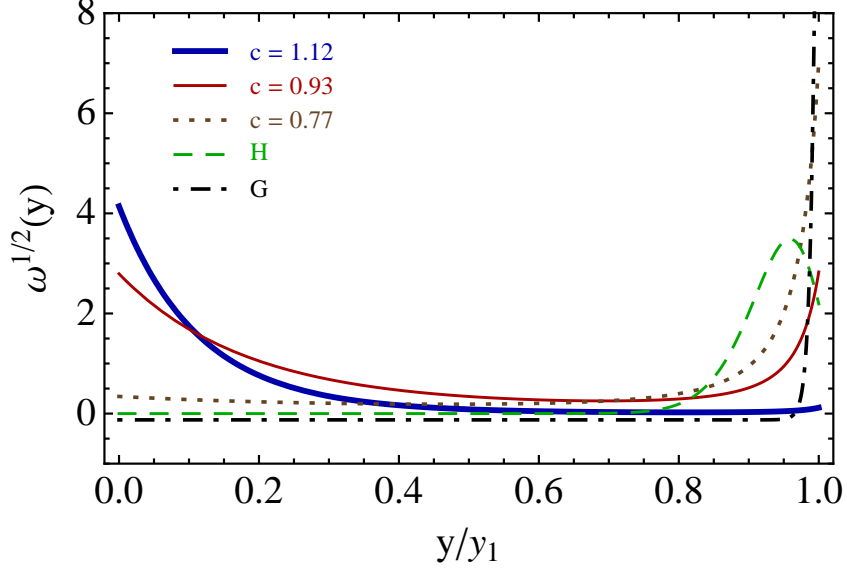


FIG. 7: Fermion zero-mode, Higgs and first gauge KK mode profiles, $\sqrt{\omega}(y)$ for $\nu = 0.4$ and $kL_1 = 0.2$.

of ≈ 114 GeV) and the value of the IR scale \tilde{k}_{eff} . We then fix the Higgs mass to its value at the minimum and compute the bound on \tilde{k}_{eff} by requiring $\Delta\chi^2 = 3.84$ (95% CL for one degree of freedom). The resulting value of the first gauge boson KK mode mass (see Fig. 1) is plotted as a function of ν for different values of kL_1 . We see that masses as light as ~ 1 TeV are allowed for $kL_1 = 0.2$ and $\nu \sim 0.45$. This plot reproduces the results presented in [13] up to small differences ($\lesssim 100$ GeV), due to the different fit procedure.

The reason for the reduced lower bound on the mass of the gauge KK modes, compared to the pure AdS_5 background, despite the absence of custodial symmetry in the model, is easy to understand. In the AdS_5 case, the warp factor forces the gauge boson KK modes to be localized close to the IR brane, where the Higgs is also localized. The large overlap then makes the mixing between the gauge boson zero-mode and massive KK-modes large (the red square in Fig. 5). The light fermions on the other hand are localized towards the UV brane and therefore their coupling to the gauge boson KK modes (the blue dot) is typically small. This is the reason for the usual enhancement of the \hat{T} parameter ($\hat{\alpha}$ is proportional to the gauge mixing squared) over the \hat{S} parameter, and of \hat{S} over W and Y . The departure from the AdS_5 background has several effects that go in the right direction to improve the EWPT. The first

ton FB asymmetries (8), heavy flavor (6), effective $\sin^2\theta_W$ (2), and 8 leptonic/strange quark polarization asymmetries. We do not fit the SM parameters, but only those associated with the new KK physics.

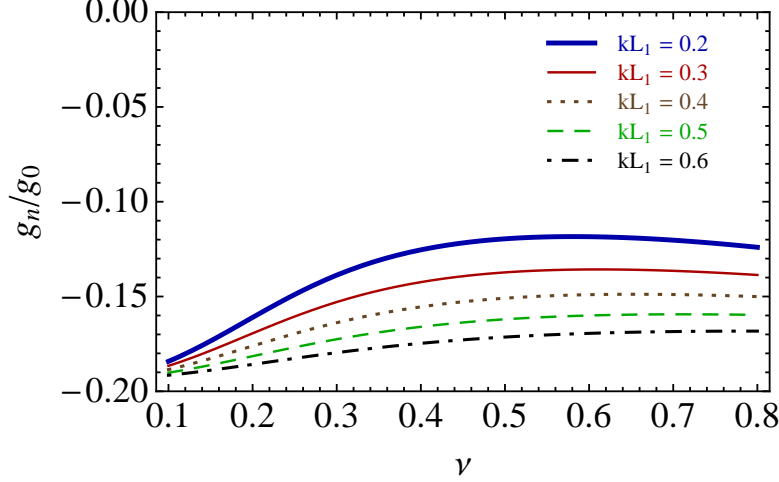


FIG. 8: Couplings of UV localized fermions to the first-level KK gauge bosons, in units of the zero-mode gauge coupling. We show curves as a function of ν , and for different values of kL_1 .

is that the KK gauge bosons are more strongly localized towards the IR brane whereas the Higgs, although localized towards the IR brane, reaches a maximum *before* the IR brane [the “physical” Higgs wavefunction is given by $\sqrt{\omega_h(y)} \approx e^{-A(y)} e^{aky}$, and the suppression near the IR brane arises from the nearby singularity in $A(y)$]. This reduces, sometimes dramatically, the gauge mixing through the Higgs vev, and therefore the contribution to the \hat{T} parameter (and somewhat less the \hat{S} parameter). This effect can be observed in Fig. 7, in which we show the “physical” profiles $\sqrt{\omega}$ of Eq. (24), for the Higgs, the first gauge KK mode, and for bulk fermion zero-modes with three different values of the bulk masses. The maximum of the Higgs profile before the IR brane is evident, together with the very strong localization of the first gauge KK mode, leading to a reduced value of the relevant overlap integral.

The second effect of the warp factor is that the coupling of UV localized fermions to gauge KK modes is reduced with respect to the standard AdS_5 case. This further reduces the \hat{S} parameter (but will also have a negative impact on collider searches). In Fig. 8 we show the value of the coupling of UV localized fermions to the first gauge boson KK mode (in units of $g_0 = g_5/\sqrt{y_1}$) for different values of ν and kL_1 . Only for small values of ν and large values of kL_1 does one approach the coupling of the AdS_5 background. Note that for the values preferred by the EWPT (see Fig. 6) this coupling is reduced to almost half the AdS_5 value.

C. The Effects of the Third Generation

Let us now consider the effect of the third quark generation. We consider three bulk fermion fields with the following quantum numbers under the $SU(2)_L \times U(1)_Y$ gauge group and BC

$$Q = (2, 1/6) \sim [++] , \quad T = (1, 2/3) \sim [--] , \quad B = (1, -1/3) \sim [--] , \quad (32)$$

with localization parameters c_Q , c_T and c_B , respectively. For fixed values of these localization parameters we can choose the 5D Yukawa couplings so that the top and bottom masses are reproduced. Due to the upper bound on Y_5 , the top mass cannot be generated if the Q and T zero-modes are far from the IR brane. The LH bottom, which is in the zero-mode of Q , can then receive large corrections to its couplings, from gauge and fermion KK modes. Anomalous contributions to the $Zb_L\bar{b}_L$ coupling can therefore impose stringent constraints in warped models without custodial protection. The general expression for the *tree-level* correction to the $Zb_L\bar{b}_L$ coupling induced by the gauge boson KK modes is given in [21]. For our model it reads

$$\delta g_{b_L} = -\frac{g^2 v^2}{2c_W^2} \left[\frac{g^2}{2} + \frac{g'^2}{6} \right] (\hat{\beta}_Q - \hat{\beta}_{UV}) , \quad (33)$$

where the term proportional to $\hat{\beta}_{UV}$ corresponds to the universal part that is absorbed in the oblique parameters. To this we have to add the *tree-level* fermionic contribution, that we have computed exactly by diagonalizing numerically the KK fermion mass matrix, and computing the resulting coupling to the Z of the lightest mass eigenstate (the bottom quark). We will consider the 1-loop effects separately.

In order to test the dependence of the constraints on the assumptions on the 5D Yukawa coupling we have taken the following benchmark scenarios. For each value of ν and kL_1 and each value of c_Q we fix c_T so that the top mass is reproduced (including the effect of the mixing with fermion KK modes) assuming that $Y_5^t = Y_5^{\max}$ (**scenario 1**). We note that, due to the maximum of the Higgs profile, there is a fixed value of c_T for which the overlap is maximal and therefore the 5D Yukawa coupling is minimal. Therefore, we also consider the case that Y_5^t is the minimal one for which it is possible to reproduce the correct top mass (**scenario 2**). Regarding the bottom sector, we consider three different scenarios by fixing the 5D bottom Yukawa to $Y_5^b = Y_5^t$ (**scenario a**), $Y_5^b = Y_5^t/5$ (**scenario b**), $Y_5^b = Y_5^t/10$ (**scenario c**). Scenario *a* assumes exact anarchy whereas in the other two we allow for deviations between different Yukawas.

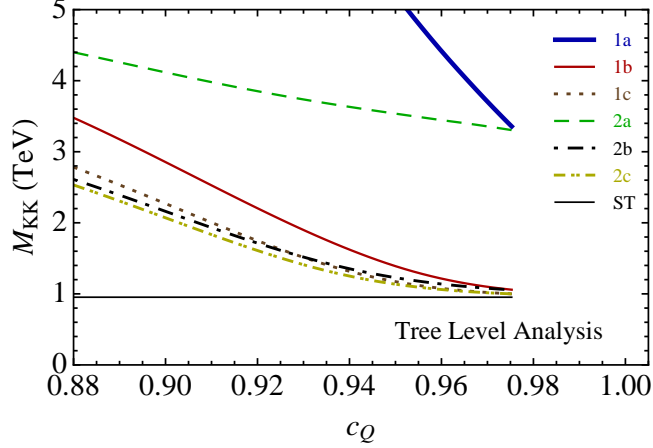


FIG. 9: Tree-level 95% CL lower bound on the mass of the first gauge KK mode as a function of the localization of the LH top/bottom multiplet (c_Q) for the six scenarios discussed in the text. We fix $\nu = 0.4$ and $kL_1 = 0.2$. The lines end at the value of c_Q beyond which the top mass cannot be generated. For comparison we also show the result of the fit if the effects of third generation quarks are neglected (horizontal “ST” line). The maximal delocalization is obtained for $c \approx 0.93$ (see Fig. 2).

We have studied the tree-level effect of third generation quarks on EWPT by performing a scan over ν and kL_1 . For each value of these parameters, we have computed the maximum value of c_Q that allows to generate the top mass (i.e. the furthest from the IR brane). We have then scanned over the values of c_Q smaller than this maximal value for the six different scenarios (1a, 1b, 1c, 2a, 2b, 2c) described above. The fit has been performed as in the case of the gauge contribution, described in the previous subsection, but including now the constraint from the $Zb_L\bar{b}_L$ coupling described above. Fixing c_Q and marginalizing over the Higgs mass, we find the value of \tilde{k}_{eff} that gives $\Delta\chi^2 = 3.84$, corresponding to 95% CL for one degree of freedom. In all cases the preferred value of the Higgs mass is close to its current lower limit $m_h \approx 114$ GeV. We show in Fig. 9 a sample result for $\nu = 0.4$ and $kL_1 = 0.2$. We display, based on a tree-level analysis, the 95% CL lower bound on the mass of the first gauge KK mode as a function of c_Q for all six scenarios, and also the result of the fit when all fermions are localized on the UV brane as considered in [13] (horizontal line denoted by ST in the plot). It is clear that the bound is very sensitive to the value of the localization of the LH top/bottom doublet as expected for a non-custodial model. The correction is smaller for a larger c_Q (the LH top/bottom further

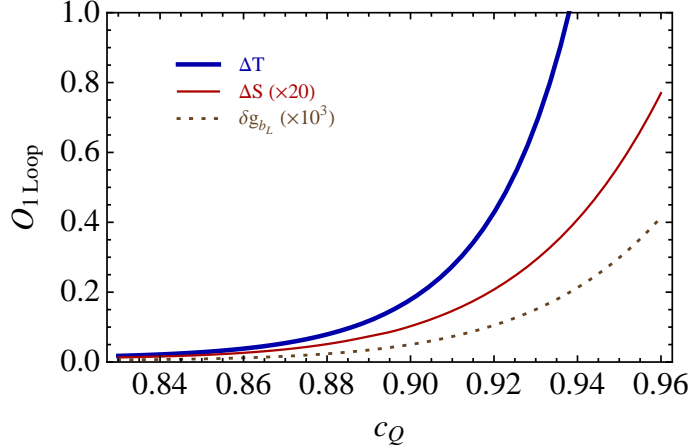


FIG. 10: One-loop contribution to T , S and δg_{b_L} , as a function of c_Q , in scenario 2c (see text). We take $\nu = 0.4$, $kL_1 = 0.2$ and $\tilde{k}_{\text{eff}} = 1$ TeV (which corresponds to $M_{\text{KK}} \approx 2.3$ TeV).

from the IR brane). The non-trivial result we find is that the top mass (just barely) allows c_Q to be large enough to make the corrections to the $Zb_L\bar{b}_L$ coupling negligible (the lines in the figure end at the point of c_Q beyond which the top mass cannot be generated). Unfortunately, loop effects change this conclusion, as discussed below. The other property that is clear from the plot is that exact anarchy (scenarios 1a and 2a) is extremely constrained by EWPT. The reason is that the Yukawa couplings in the bottom sector are very large and the mixing with the bottom KK modes induces very large corrections to the $Zb_L\bar{b}_L$ coupling. However, we see that a suppression in the 5D bottom Yukawa by a factor of 5 is already enough to get the bound on the scale of new physics reasonably low. We have also checked that the $\bar{t}_R\gamma^\mu b_R W_\mu^+$ coupling is in these cases typically $\lesssim 10^{-4}$ (in units of $g/\sqrt{2}$) and should therefore cause no trouble with $b \rightarrow s\gamma$ constraints [25] (a full analysis, including the fermion KK modes in the calculation, to properly account for this constraint, is beyond the scope of this paper).

As mentioned in Subsection IV A, the 1-loop contributions to T , S and δg_{b_L} are finite (while at two-loop order, they are logarithmically divergent). We have computed these one-loop effects using the methods described in [7], and show a numerical example in Fig. 10. Here we have taken a gravitational background with $\nu = 0.4$ and $kL_1 = 0.2$, and we have assumed scenario 2c defined above, with $\tilde{k}_{\text{eff}} = 1$ TeV. Recall that scenarios 2 are such that the 5D Yukawa coupling is the minimal one that still allows to reproduce the top quark mass, for given c_Q . In this sense, these scenarios minimize the size of these one-loop effects, which are controlled by this coupling.

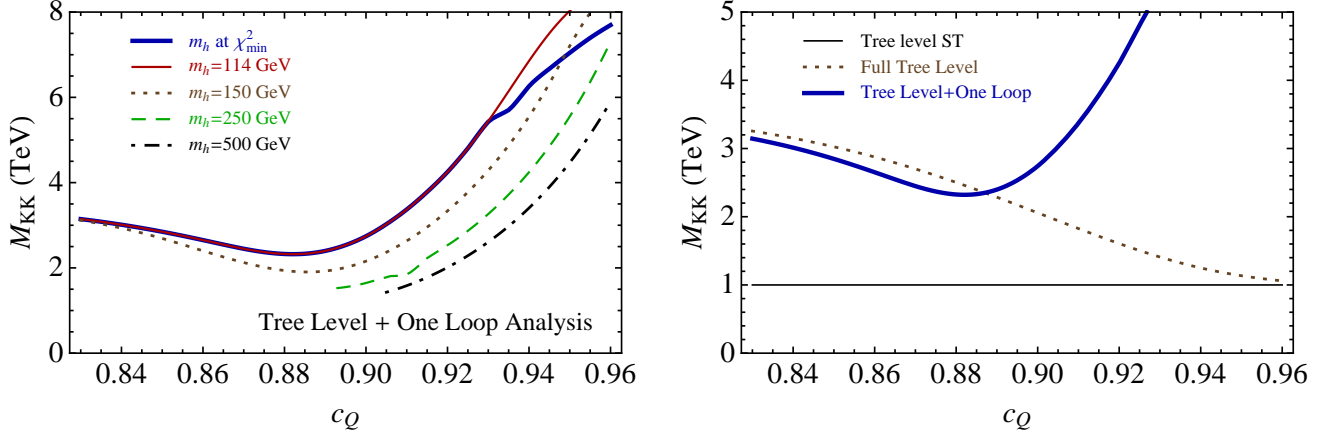


FIG. 11: Left panel: 95% CL lower bound on the mass of the first gauge KK mode as a function of the localization of the LH top/bottom multiplet (c_Q) in scenario 2c, including one-loop effects. The different lines correspond to different values of m_h , with the one marked as “ m_h at χ^2_{\min} ” corresponding to marginalization over m_h . The curves are terminated where the goodness-of-fit gives a 5% likelihood. Right panel: comparison of the tree-level oblique, full tree-level, and tree-level plus 1-loop bounds on M_{KK} , assuming marginalization over m_h . In all cases, we fix $\nu = 0.4$ and $kL_1 = 0.2$.

We see in the figure that the 1-loop contribution to the T parameter can be significant, and imposes an upper bound on c_Q that is stronger than the one coming from the top mass itself. By contrast, the 1-loop contributions to S and δg_{b_L} are relatively small (in the figure we show $20 \times S$ and $10^3 \times \delta g_{b_L}$). This constraint is in tension with the one due to the (tree-level) modification of the $Zb_L\bar{b}_L$ coupling. We show in the left panel of Fig. 11 the resulting lower bound on the KK-gluon mass corresponding to **scenario 2c**. The thick solid (blue) line corresponds to the fit procedure used at tree-level, i.e. evaluating $\Delta\chi^2 = 3.84$ with a Higgs mass that minimizes the total χ^2 (typically near the LEP Higgs bound). However, we also show the bounds on the KK scale assuming other fixed values of the Higgs mass (as would be appropriate if a Higgs of such a mass was actually discovered). We see from the thick solid blue curve that –marginalizing over m_h – a lower 95% CL bound of $M_{KK} \approx 2.3$ TeV is found for $c_Q \approx 0.88$. We note that for this c_Q one has $\chi^2_{\min}/\text{dof} = 25.6/24$ at $(m_h, M_{KK}) = (114 \text{ GeV}, 4.3 \text{ TeV})$, which gives a goodness-of-fit with 37% likelihood. This results mainly from a compromise between the (tree-level) δg_{b_L} and the 1-loop contribution to T . However, the black dot-dashed line shows that for a heavier Higgs, with fixed $m_h = 500$ GeV, a KK-gluon as light as 1.5 TeV (1.4 TeV) would be possible, which corresponds to the 95% CL contour about a best fit point

with $\chi^2_{\min}/\text{dof} = 34/25$ ($\chi^2_{\min}/\text{dof} = 37.6/25$) leading to a 10% (5%) likelihood. Thus, it may be possible to have warped models with KK-gluons around 1.5 TeV that fit the EW data reasonably well. As a summary plot that highlights the impact of the various contributions to the EW observables discussed above, we show in the right panel of Fig. 11 the bounds on the KK-gluon mass, as a function of c_Q , for the EWPT fits at a) tree-level in the oblique approximation [thin solid black line], b) full tree-level [dotted brown line] and c) tree level plus 1-loop [thick solid blue line]. In all cases we marginalize over m_h , although as just pointed out this may lead to an overly pessimistic conclusion in regards to how low M_{KK} could actually be. At any rate, it is clear from this figure that both the corrections to the $Zb_L\bar{b}_L$ coupling and the one-loop effects play an important role in determining the allowed M_{KK} .

We also point out that the models consistent with the EWPT up to 1-loop order, which have a relatively low M_{KK} , always have KK-fermion Yukawa couplings that are *perturbative*. For instance, at the minimum of the solid thick blue curve in Fig. 11, with $M_{\text{KK}} \approx 2.3$ TeV, the 4D Yukawa couplings of the form $h\bar{Q}_L^{(n)}t_R^{(n)}$ are all $\mathcal{O}(1)$, while the off-diagonal ones (i.e. coupling different KK levels) are much less than one (becoming smaller the further apart the masses of the two KK modes).⁷ This is a result of the suppression in overlap integrals associated with the non-trivial profile of the Higgs field, much as in the KK-gauge/Higgs couplings illustrated in Fig. 7. Thus, higher order (divergent) effects involving additional powers of Yukawa couplings are expected to be suppressed. The most important effects that remain are associated with QCD higher-order corrections, as mentioned in Subsection IV A. Thus, the above results should be taken as an illustration of how light the KK resonances can reasonably be, as far as the EW precision constraints are concerned.

These results have important implications for collider searches. First, the absence of custodial symmetry implies a quite minimal spectrum of massive modes. In particular, very light fermions [10, 11], natural in custodial models are not expected in the model under study. We show in Fig. 12 the mass of the first fermion KK mode of a $[++]$ field as a function of the localization parameter c for different values of ν and kL_1 . These figures, together with Fig. 1

⁷ By contrast, scenarios 1 have diagonal 4D Yukawa couplings for the KK fermions of order 3 – 4, and always lead to a very large 1-loop contribution to T , unless M_{KK} is above $\mathcal{O}(10 \text{ TeV})$. In such cases, higher-order contributions associated with the Yukawa interactions may not be suppressed, and can have a large impact on the EW analysis. Nevertheless, barring tuned cancellation between these and the UV contributions, one expects that the KK resonances will be out of the LHC reach in such scenarios.

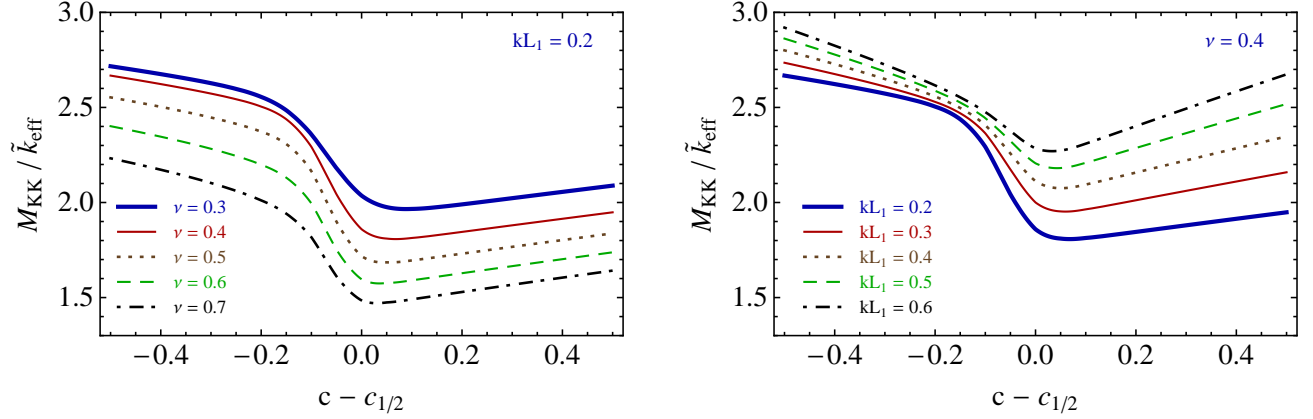


FIG. 12: Mass of the first fermion KK mode for a $[++]$ field in units of \tilde{k}_{eff} as a function of its localization parameter (with respect to the mostly delocalized value) for values of $\nu = 0.3, 0.4, 0.5, 0.6, 0.7$ (top to bottom, left panel) and $kL_1 = 0.2, 0.3, 0.4, 0.5, 0.6$ (bottom to top, right panel).

show that, in some cases, the first KK gluon can decay into a top (or bottom) and a heavy fermion, although the latter are in this case much closer to threshold than in custodial models. Channels with a heavy fermion of the first and second generations are also typically open: under the anarchic assumption such decay channels are very suppressed, but they could be more important in other scenarios for flavor. Second, masses lighter than previously considered in models with warped extra dimensions (with semi-anarchic Yukawas) may be allowed by EWPT. This result is very sensitive to the localization of the third generation quarks which determine the coupling of the top and bottom quarks to the gauge KK modes, as well as the KK-fermion Yukawa couplings. We show in Fig. 13 the couplings of the different quarks to the first KK gluon in units of $g_0 = g_5/\sqrt{y_1}$ for scenarios 2, with $\nu = 0.4$ and $kL_1 = 0.2$. We see that the largest is the coupling to $t_R \bar{t}_R$, followed by $Q_L \bar{Q}_L$ and then to light quark pairs. Thus, the KK-gluon decays dominantly into RH top pairs (or, perhaps, a channel involving one KK-fermion and the associated zero-mode), bearing some resemblance to the scenario of Eq. (1). However, the reduced couplings to the light quarks can make the discovery more challenging, for a given M_{KK} .

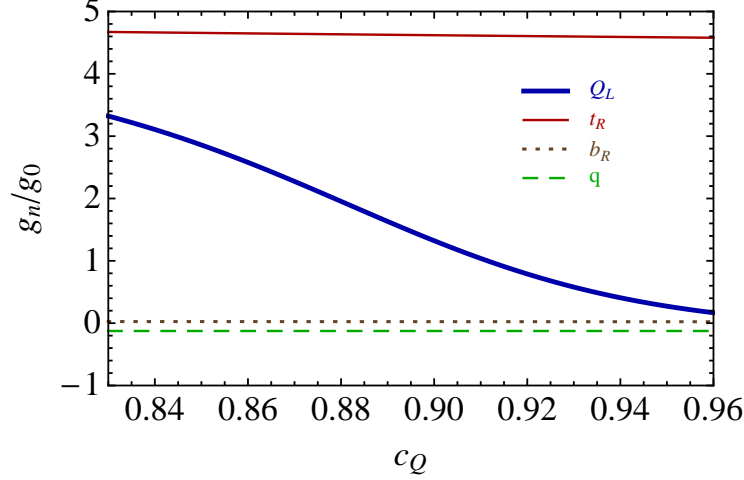


FIG. 13: Couplings to the first gauge KK mode (in units of $g_0 = g_5/\sqrt{y_1}$) of the third generation LH quarks Q_L , RH top t_R , RH bottom b_R , and light quarks q , as a function of c_Q , for scenario 2 (sub-scenarios a , b and c give similar results for the couplings). We fix $\nu = 0.4$ and $kL_1 = 0.2$. The localization parameters c_T , c_B and the top and bottom masses have been fixed as described in the text. The b_R and q couplings are almost identical.

V. PHENOMENOLOGICAL IMPLICATIONS

In this section we present the main collider implications of some selected points in parameter space. As we have seen in the previous section, the EW fit prefers models of type **2**, which always have the KK-gluons relatively strongly coupled to t_R (see Figs. 11 and 13). Thus, the $t\bar{t}$ decay channel for the KK-gluon is always dominant. To illustrate the expected signal at the LHC, we consider two models, as suggested by the analysis in the previous section.

The first one corresponds to scenario **2c** with $\nu = 0.4$, $kL_1 = 0.2$ and $c_Q = 0.88$. With $m_h = 114$ GeV, we find a $\chi^2/\text{dof} = 25.6/24$, giving a likelihood of 37%. This fit is only slightly worse than the SM one: the total χ^2 is slightly reduced, but there is one additional degree of freedom, corresponding to \tilde{k}_{eff} . The KK gluon mass is

$$M_{\text{KK}} \approx 2.3 \text{ TeV} \quad (95\% \text{ CL}) . \quad (34)$$

We also find that the first KK resonance of the third generation quark $SU(2)_L$ doublet has a mass $M_Q \approx 2.1$ TeV, while the first KK resonance of the bottom $SU(2)_L$ singlet has a mass $M_B \approx 1.85$ TeV. Both are sufficiently light for the decays $G^{(1)} \rightarrow Q_L^{(0)} \bar{Q}_L^{(1)}$ and $G^{(1)} \rightarrow b_R^{(0)} \bar{B}_R^{(1)}$

to be open. The corresponding couplings to fermion pairs are

$$g_{Q_L} \approx 1.95g_s, \quad g_{t_R} \approx 4.63g_s, \quad g_{b_R} \approx 0.02g_s, \quad g_q \approx -0.13g_s, \quad (35)$$

$$g_{q_L, Q_L^{(1)}} \approx 3.85g_s, \quad g_{b_R, B_R^{(1)}} \approx 1.15g_s, \quad (36)$$

where we omitted the superscripts for the zero modes, and the first line refers to SM fermion pairs. The first KK-resonance of the top $SU(2)_L$ singlet is heavier than the KK-gluon, so that this channel is kinematically closed. However, the first KK resonances of all the remaining SM fermions are lighter than the KK-gluon, and are therefore open as decays of the form $G^{(1)} \rightarrow q^{(0)}q^{(1)}$. Nevertheless, the relevant couplings are all significantly smaller than g_s , so that these are somewhat rare decays that, in spite of the multiplicity, do not change appreciably the width of the KK-gluon. With the above couplings, we find that $\Gamma_{G^{(1)}} \approx 710$ GeV, and that the KK-gluon has the following branching fractions:

$$BR(G^{(1)} \rightarrow t\bar{t}) \approx 0.81, \quad BR(G^{(1)} \rightarrow b\bar{b}) \approx 0.12, \quad BR(G^{(1)} \rightarrow q\bar{q}) \approx 0.004, \quad (37)$$

$$BR(G^{(1)} \rightarrow t_L^{(1)}t) \approx 0.02, \quad BR(G^{(1)} \rightarrow b_L^{(1)}b) \approx 0.04, \quad BR(G^{(1)} \rightarrow b_R^{(1)}b) \approx 0.01, \quad (38)$$

where in the last line both conjugate processes (e.g. $G^{(1)} \rightarrow t_L^{(1)}\bar{t}$ and $G^{(1)} \rightarrow \bar{t}_L^{(1)}t$) are understood. The total $G^{(1)}$ production cross section is ~ 24 fb (~ 188 fb) at a CM energy of 7 TeV (14 TeV).

The second model has instead $c_Q = 0.906$ which, with $m_h = 500$ GeV, leads to $\chi^2/\text{dof} = 34/25$, giving a likelihood of 10% (still reasonably large). The KK-gluon mass is now

$$M_{KK} \approx 1.5 \text{ TeV} \quad (95\% \text{ CL}), \quad (39)$$

while the first KK resonance of the third generation quark $SU(2)_L$ doublet has a mass $M_Q \approx 1.3$ TeV, and the first KK resonance of the bottom $SU(2)_L$ singlet has a mass $M_B \approx 1.2$ TeV. The corresponding couplings to fermion pairs are

$$g_{Q_L} \approx 1.17, \quad g_{t_R} \approx 4.62, \quad g_{b_R} \approx -0.03g_s, \quad g_q \approx -0.13g_s, \quad (40)$$

$$g_{q_L, Q_L^{(1)}} \approx 3.16g_s, \quad g_{b_R, B_R^{(1)}} \approx 1.15g_s. \quad (41)$$

Now we have $\Gamma_{G^{(1)}} \approx 390$ GeV and the following branching fractions:

$$BR(G^{(1)} \rightarrow t\bar{t}) = 0.83, \quad BR(G^{(1)} \rightarrow b\bar{b}) = 0.05, \quad BR(G^{(1)} \rightarrow q\bar{q}) = 0.005, \quad (42)$$

$$BR(G^{(1)} \rightarrow t_L^{(1)}t) \approx 0.03, \quad BR(G^{(1)} \rightarrow b_L^{(1)}b) \approx 0.06, \quad BR(G^{(1)} \rightarrow b_R^{(1)}b) \approx 0.02. \quad (43)$$

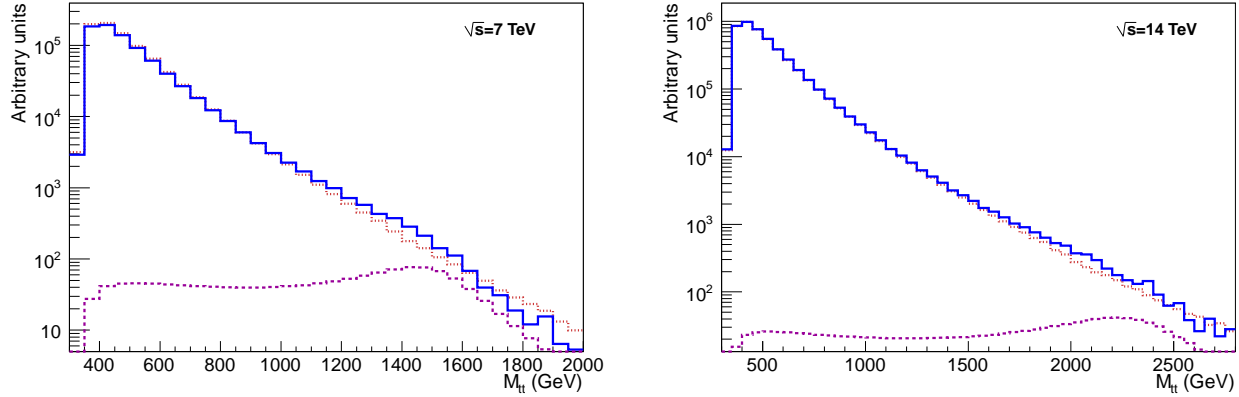


FIG. 14: $t\bar{t}$ invariant mass distribution in the SM (red dotted), in the model with extra-dimensional physics (solid blue) and the contribution of just the KK gluon exchange (dashed purple). The left panel corresponds to a KK-gluon with $M_{\text{KK}} \approx 1.5$ TeV and the couplings of Eqs. (40)-(41). The right panel corresponds to $M_{\text{KK}} \approx 2.3$ TeV and the couplings of Eqs. (35)-(36).

The total $G^{(1)}$ production cross section is ~ 0.19 pb (~ 1.3 pb) at a CM energy of 7 TeV (14 TeV).

The BR's in these models are relatively similar to the benchmark of Ref. [5], but with lighter masses and reduced couplings to the light quarks. Note, however, that the first model has a non-negligible branching fraction into bottom pairs, and that there are “exotic” channels involving a KK fermion with BRs at the few percent level (in the case of the third generation; for the first two generations the corresponding BRs are expected to be much smaller, although the precise values depend on the details of how flavor is implemented).

We have implemented these models in MADGRAPH/MADEVENT v4 [26], using PYTHIA 6 [27] for hadronization and showering and PGS4 [28] for detector simulation. We use the **CTEQ6L1** parton distribution function, with the QCD renormalization and factorization scales equal to the central m_T^2 of the event. We have then implemented the $t\bar{t}$ CMS analysis of Ref. [29], which we use to normalize our SM sample, generated by MG/ME, once we check that the shape of the $t\bar{t}$ invariant mass distribution is reasonably reproduced. We use this (re)normalization factor for the signal + background, taking into account interference effects. We consider here the semi-leptonic $t\bar{t}$ channel, separating the e and μ channels [29]. We show in Fig. 14 the expected $t\bar{t}$ invariant mass distribution at the LHC, at the partonic level. The left (right) panel corresponds to the second (first) model above at $\sqrt{s} = 7$ TeV ($\sqrt{s} = 14$ TeV). In both plots we

represent the SM prediction with a red dotted line and the prediction of the model (including the interference with the SM $t\bar{t}$ contribution) in solid blue. Also, just to guide the eye, we show the contribution assuming only the KK gluon exchange as a purple dashed line. Although the lightest mass case shows a slight excess over background, these results suggest that extracting the signal will be challenging.

VI. CONCLUSIONS

We have studied a recently proposed model in five dimensions with a warped background [13] that can be consistent –from the point of view of EW precision constraints– with new gauge boson resonances at about 1.5 TeV. This represents a significant reduction of the bound on the new physics scale compared to fairly elaborate models based on AdS_5 backgrounds. The scenario is also relatively simple, with just the SM field content promoted to 5D, plus a new “stabilizing” scalar field that is responsible for the all-important deviation from AdS_5 near the IR brane. A simple way to understand the relaxation of the bound can be obtained by considering the localization of the relevant fields: the gauge boson KK modes are strongly attracted towards the IR brane, while it is still possible to accommodate a profile for the Higgs field that, although mostly IR localized (so that the RS solution to the hierarchy problem is preserved), attains its maximum before reaching the IR brane. As a result, any overlap integral that involves the Higgs and the (first) gauge or fermion KK modes can be dramatically reduced compared to cases where all the fields are localized within a distance of order $1/k$ from the IR brane, as happens in the AdS_5 background. Since the deviations from the SM are determined by such overlap integrals (and the scale of the new resonances), lighter states can be allowed.

Here we have extended the study in Ref. [13] to the case where the SM fermions can be arbitrarily localized along the extra-dimension, which allows to understand the SM flavor structure as arising from the localization of fermion fields. We point out that reproducing the observed top quark mass, which requires the top quark to be localized sufficiently close to the IR brane, can result in significant constraints from anomalous contributions to the $Zb_L\bar{b}_L$ coupling, beyond the constraints from the oblique parameters considered in Ref. [13]. This is a direct consequence of the absence of any custodial protection [4] together with the “anarchical” explanation of flavor. In addition, we find that the 1-loop corrections to the EW observables, which are finite in these scenarios, strongly restrict the allowed region of parameter space. In

particular, a tension between the (tree-level) corrections to the $Zb_L\bar{b}_L$ coupling and the 1-loop contribution to the Peskin-Takeuchi T -parameter, strongly constrains the localization of the third generation quarks and the resulting 95% CL bound on the KK scale. Nevertheless we find that for an optimal top/bottom $SU(2)_L$ doublet localization, and when the 5D bottom Yukawa coupling is a factor of a *few* smaller than the top one, the KK-gluons can be as light as 1.5 TeV if the Higgs is heavy, with the likelihood inferred from the EW fit still being reasonably large. However, if the Higgs mass is allowed to float in the fit, one finds a 95% CL lower bound of $M_{\text{KK}} \approx 2.3$ TeV,

A KK-gluon mass of about 1.5 TeV can open the exciting possibility that the Randall-Sundrum solution to the hierarchy problem, based on warped compactifications, and with a bulk SM field content, could lead to observable resonances at the LHC with lower luminosities than previously thought. Compared to the widely studied AdS_5 framework, the result arises from two opposing effects: the previously mentioned strong localization of the gauge boson resonances towards the IR brane implies a reduction of its couplings to the light fermions, thus leading to a suppression in production. This can be compensated by the lower allowed mass of the gauge KK modes. However, we find that discovering such a resonance in the dominant $t\bar{t}$ channel is likely to be challenging. Boosted top techniques and a very detailed knowledge of the $t\bar{t}$ tail will likely be required to discover these modes. We also find that, unlike in the case of an AdS_5 background without the custodial symmetry, the present class of models allows for the production of single KK-fermion resonances of the SM fields, in KK-gluon decays. Although these decay channels are likely subdominant (in particular, they do not dramatically change the KK-gluon width), they may provide an interesting handle on the fermionic resonances.⁸ Nevertheless, rather high luminosities are likely necessary. One should recall, however, that we are working under the (semi-)anarchic assumption of flavor. If the light families are closer to the IR brane (with a correspondingly smaller 5D Yukawa coupling) the production cross section can be larger, and relatively light spin-1 resonances in the 1-2 TeV range could be more readily observed at the LHC.

⁸ Note that in models with custodial symmetry, fermion custodians are expected to be in general lighter and these channels are likely to be more relevant [32, 33]. The discovery of new fermions with exotic charges, like $Q = 5/3$ [10, 11], would in any case be a clear smoking gun of custodial models.

Acknowledgments

We would like to thank Kaustubh Agashe, Mert Aybat, Cédric Delaunay, Gero von Gersdorff and especially Manuel Pérez-Victoria for useful discussions. A.C. and J.S. are supported by MICINN (FPA2006-05294, FPA2010-17915, FPU and Ramón y Cajal programs) and Junta de Andalucía (FQM 101, FQM 03048 and FQM-6552). E.P. is supported by DOE grant DE-FG02-92ER40699.

-
- [1] L. Randall, R. Sundrum, Phys. Rev. Lett. **83** (1999) 3370-3373. [hep-ph/9905221]; Phys. Rev. Lett. **83** (1999) 4690-4693. [hep-th/9906064].
 - [2] M. E. Peskin and T. Takeuchi, Phys. Rev. D **46**, 381 (1992).
 - [3] S. J. Huber, C. -A. Lee, Q. Shafi, Phys. Lett. **B531** (2002) 112-118. [hep-ph/0111465].
 - [4] K. Agashe, A. Delgado, M. J. May, R. Sundrum, JHEP **0308** (2003) 050. [hep-ph/0308036]; K. Agashe, R. Contino, L. Da Rold, A. Pomarol, Phys. Lett. **B641** (2006) 62-66. [hep-ph/0605341].
 - [5] K. Agashe, A. Belyaev, T. Krupovnickas, G. Perez and J. Virzi, Phys. Rev. D **77**, 015003 (2008) [arXiv:hep-ph/0612015]; B. Lillie, L. Randall and L. T. Wang, JHEP **0709** (2007) 074 [arXiv:hep-ph/0701166]; A. Djouadi, G. Moreau, R. K. Singh, Nucl. Phys. **B797**, 1-26 (2008). [arXiv:0706.4191 [hep-ph]].
 - [6] M. S. Carena, A. Delgado, E. Pontón, T. M. P. Tait and C. E. M. Wagner, Phys. Rev. D **68** (2003) 035010 [arXiv:hep-ph/0305188]; Phys. Rev. D **71** (2005) 015010 [arXiv:hep-ph/0410344]; A. Djouadi, G. Moreau and F. Richard, Nucl. Phys. B **773** (2007) 43 [arXiv:hep-ph/0610173].
 - [7] M. S. Carena, E. Pontón, J. Santiago and C. E. M. Wagner, Nucl. Phys. B **759** (2006) 202 [arXiv:hep-ph/0607106]; Phys. Rev. D **76** (2007) 035006 [arXiv:hep-ph/0701055].
 - [8] C. Delaunay, O. Gedalia, S. J. Lee, G. Perez, E. Pontón, Phys. Rev. **D83**, 115003 (2011). [arXiv:1007.0243 [hep-ph]]; arXiv:1101.2902 [hep-ph].
 - [9] A. L. Fitzpatrick, J. Kaplan, L. Randall, L. -T. Wang, JHEP **0709** (2007) 013. [hep-ph/0701150]; K. Agashe, H. Davoudiasl, G. Perez, A. Soni, Phys. Rev. **D76** (2007) 036006. [hep-ph/0701186]; K. Agashe *et al.*, Phys. Rev. D **76** (2007) 115015 [arXiv:0709.0007 [hep-ph]]; K. Agashe, S. Gopalakrishna, T. Han, G. Y. Huang and A. Soni, Phys. Rev. D **80** (2009) 075007

- [arXiv:0810.1497 [hep-ph]]; K. Agashe, A. Azatov, T. Han, Y. Li, Z. G. Si and L. Zhu, Phys. Rev. D **81** (2010) 096002 [arXiv:0911.0059 [hep-ph]].
- [10] G. Cacciapaglia, C. Csaki, G. Marandella and J. Terning, Phys. Rev. D **75** (2007) 015003 [arXiv:hep-ph/0607146]; R. Contino, L. Da Rold and A. Pomarol, Phys. Rev. D **75** (2007) 055014 [arXiv:hep-ph/0612048]; A. D. Medina, N. R. Shah and C. E. M. Wagner, Phys. Rev. D **76** (2007) 095010 [arXiv:0706.1281 [hep-ph]]; A. Pomarol and J. Serra, Phys. Rev. D **78** (2008) 074026 [arXiv:0806.3247 [hep-ph]].
- [11] R. Contino and G. Servant, JHEP **0806** (2008) 026 [arXiv:0801.1679 [hep-ph]]; A. Atre, M. Carena, T. Han and J. Santiago, Phys. Rev. D **79** (2009) 054018 [arXiv:0806.3966 [hep-ph]]. J. A. Aguilar-Saavedra, JHEP **0911** (2009) 030 [arXiv:0907.3155 [hep-ph]]; J. Mrazek and A. Wulzer, Phys. Rev. D **81** (2010) 075006 [arXiv:0909.3977 [hep-ph]]; F. del Aguila, A. Carmona and J. Santiago, JHEP **1008** (2010) 127 [arXiv:1001.5151 [hep-ph]]; Phys. Lett. **B695** (2011) 449-453. [arXiv:1007.4206 [hep-ph]]; G. Dissertori, E. Furlan, F. Moortgat, P. Nef, JHEP **1009** (2010) 019. [arXiv:1005.4414 [hep-ph]]; A. Atre, G. Azuelos, M. Carena, T. Han, E. Ozcan, J. Santiago, G. Unel, [arXiv:1102.1987 [hep-ph]].
- [12] J. Santiago, PoS **ICHEP2010** (2010) 557. [arXiv:1103.4114 [hep-ph]].
- [13] J. A. Cabrer, G. von Gersdorff, M. Quirós, Phys. Lett. **B697** (2011) 208-214 [arXiv:1011.2205 [hep-ph]]; JHEP **1105** (2011) 083 [arXiv:1103.1388 [hep-ph]]; [arXiv:1104.3149 [hep-ph]].
- [14] A. Falkowski and M. Perez-Victoria, JHEP **0812** (2008) 107 [arXiv:0806.1737 [hep-ph]]; JHEP **0912** (2009) 061 [arXiv:0901.3777 [hep-ph]].
- [15] B. Batell, T. Gherghetta and D. Sword, Phys. Rev. D **78** (2008) 116011 [arXiv:0808.3977 [hep-ph]].
- [16] S. Mert Aybat and J. Santiago, Phys. Rev. D **80** (2009) 035005 [arXiv:0905.3032 [hep-ph]]; AIP Conf. Proc. **1200** (2010) 611 [arXiv:0909.3999 [hep-ph]].
- [17] T. Gherghetta and D. Sword, Phys. Rev. D **80** (2009) 065015 [arXiv:0907.3523 [hep-ph]]; A. Delgado and D. Diego, Phys. Rev. D **80** (2009) 024030 [arXiv:0905.1095 [hep-ph]]; M. Atkins and S. J. Huber, Phys. Rev. D **82** (2010) 056007 [arXiv:1002.5044 [hep-ph]].
- [18] K. Agashe, A. Azatov, L. Zhu, Phys. Rev. **D79**, 056006 (2009). [arXiv:0810.1016 [hep-ph]].
- [19] Z. Chacko, M. A. Luty and E. Pontón, JHEP **0007**, 036 (2000) [arXiv:hep-ph/9909248].
- [20] R. Barbieri, A. Pomarol, R. Rattazzi and A. Strumia, Nucl. Phys. B **703** (2004) 127

- [arXiv:hep-ph/0405040].
- [21] H. Davoudiasl, S. Gopalakrishna, E. Pontón, J. Santiago, New J. Phys. **12** (2010) 075011. [arXiv:0908.1968 [hep-ph]].
 - [22] H. Davoudiasl, G. Perez, A. Soni, Phys. Lett. **B665** (2008) 67-71. [arXiv:0802.0203 [hep-ph]].
 - [23] M. J. G. Veltman, Acta Phys. Polon. **B8** (1977) 475.
 - [24] Z. Han, W. Skiba, Phys. Rev. **D71** (2005) 075009. [hep-ph/0412166]; Z. Han, Phys. Rev. **D73**, 015005 (2006). [hep-ph/0510125].
 - [25] P. L. Cho, M. Misiak, Phys. Rev. **D49**, 5894-5903 (1994). [hep-ph/9310332]; K. Fujikawa, A. Yamada, Phys. Rev. **D49**, 5890-5893 (1994); G. Burdman, M. C. Gonzalez-Garcia, S. F. Novaes, Phys. Rev. **D61**, 114016 (2000). [hep-ph/9906329].
 - [26] J. Alwall *et al.*, JHEP **0709** (2007) 028 [arXiv:0706.2334 [hep-ph]].
 - [27] T. Sjostrand, S. Mrenna and P. Z. Skands, JHEP **0605** (2006) 026 [arXiv:hep-ph/0603175].
 - [28] PGS4 <http://www.physics.ucdavis.edu/~conway/research/software/pgs/pgs4-general.htm>
 - [29] CMS collaboration Note: TOP-10-007-PAS.
 - [30] A. Abdesselam, E. B. Kuutmann, U. Bitenc, G. Brooijmans, J. Butterworth, P. Bruckman de Renstrom, D. Buarque Franzosi, R. Buckingham *et al.*, EPHJA,C71,1661. 2011 **C71** (2011) 1661. [arXiv:1012.5412 [hep-ph]].
 - [31] B. Lillie, J. Shu, T. M. P. Tait, Phys. Rev. **D76**, 115016 (2007). [arXiv:0706.3960 [hep-ph]].
 - [32] M. Carena, A. D. Medina, B. Panes, N. R. Shah and C. E. M. Wagner, Phys. Rev. D **77** (2008) 076003 [arXiv:0712.0095 [hep-ph]].
 - [33] N. Vignaroli, arXiv:1107.4558 [hep-ph].